ARTICLE

A New kHz Velocity Map Ion/Electron Imaging Spectrometer for Femtosecond Time-Resolved Molecular Reaction Dynamics Studies

Zhi-gang He[a,b†], Zhi-chao Chen[a,b†], Dong-yuan Yang[a,b], Dong-xu Dai[a], Guo-rong Wu[a*] Xue-ming Yang[a]

a. State Key Laboratory of Molecular Reaction Dynamics, Dalian Institute of Chemical Physics, Dalian 116023, China
b. University of Chinese Academy of Sciences, Beijing 100049, China

(Dated: Received on February 19, 2017; Accepted on March 14, 2017)

A new velocity map imaging spectrometer is constructed for molecular reaction dynamics studies using time-resolved photoelectron/ion spectroscopy method. By combining a kHz pulsed valve and an ICCD camera, this velocity map imaging spectrometer can be run at a repetition rate of 1 kHz, totally compatible with the fs Ti:Sapphire laser system, facilitating time-resolved studies in gas phase which are usually time-consuming. Time-resolved velocity map imaging study of NH_3 photodissociation at 200 nm was performed and the time-resolved total kinetic energy release spectrum of $H+NH_2$ products provides rich information about the dissociation dynamics of NH_3. These results show that this new apparatus is a powerful tool for investigating the molecular reaction dynamics using time-resolved methods.

Key words: Photoelectron spectrum, Pump/probe, Femtosecond time-resolved

I. INTRODUCTION

Various experimental methods have been developed in the field of molecular reaction dynamics. They can generally be classified into two categories: energy-resolved measurements and time-resolved measurements. In the former method, the quantum state distribution, translational energy distribution, angular distribution, *etc.* of the final reaction products are measured. The reaction mechanism and dynamics are often indirectly inferred from the information of the final products, usually in concert with high-level theoretical calculations. Time-resolved methods, founded upon seminal work of Zewail and coworkers [1−3] directly follow the energy and/or charge flow within molecular systems during chemical reactions with ultrafast laser pulses, X-ray pulses, electron pulses, *etc.* Unified pictures involving both energy-resolved and time-resolved measurements are often required in order to provide the most detailed information on the dynamics of a reaction.

In time-resolved studies of molecular reaction dynamics, experimental methods are mainly differed in the way of probing a reaction triggered by the pump pulse, such as nonlinear optical spectroscopy and transient absorption spectroscopy in the condensed phase, laser-induced fluorescence and resonant multiphoton ionization in the gas phase, and time-resolved X-ray or electron diffraction in condensed or gas phases, time-resolved photoelectron spectroscopy (TRPES) in gas or condensed phases. Among them, the TRPES method has become a very powerful method in the molecular reaction dynamics studies, especially in the excited-state nonadiabatic dynamics studies, due to a number of practical and conceptual advantages brought by the photoionization probing method [4−19].

There are many ways to measure photoelectron spectra, including magnetic bottle spectrometer, hemispherical analyzer, cold target recoil ion momentum spectrometer, velocity map imaging (VMI) spectrometer *etc.* By combining with a fs laser system, time-resolved velocity map imaging (TRVMI) of photoelectron has become a popular way to measure the TRPES spectrum, with the capability of measuring the translational energy and angular distributions of photoelectron simultaneously [10, 17, 20, 21]. A TRVMI experiment needs taking images at many different delays, including those with very small signal. It typically takes many hours or even days to get enough statistics for data analysis. Therefore, it is very critical to increase the repetition rate of the TRVMI spectrometer in order to shorten the time needed or even make some of the experiments feasible. Commercial Ti:Sapphire fs laser systems can be run with a kHz repetition rate. However, most of the VMI spectrometers are limited to tens of hertz, due to the low frame rate of CCD cameras and sometimes also the low repetition rate of pulse valves. It is practically important to increase the repetition rate of VMI spectr-

†These authors contributed equally to this work.
*Author to whom correspondence should be addressed. E-mail: wugr@dicp.ac.cn

ometers up to kHz and to match with the fs laser systems. Suzuki and coworkers have developed a very elegant method to run VMI at 1000 frames/s (with a 512×512 pixel array) [22]. Complementary metal oxide semiconductor (CMOS) image sensor with multistage image intensifier was used to increase to frame rate of the camera, and programmable gate array circuit (FPGA) was used to perform real-time centers of gravity (COG) calculation [23] of the light spots on the phosphor screen and data transfer between the camera and a personal computer. Suzuki's method is very advanced, but also relatively complicated. In the present work, we report a newly constructed VMI spectrometer in which a combination of an Even-Lavie pulsed valve and an ICCD camera is used. With this simple modification, charged particles can be recorded at a frame rate of 1 kHz with a 1024×1024 pixel array. Although the readout rate is only limited to the order of 10 Hz and the real-time COG calculation is infeasible with current configuration, the 1 kHz imaging on the MCP/phosphor screen is collected with a high efficiency, without noise problem inherent to long exposure method which is often implemented when a low frame rate camera is used. The abandonment of COG calculation makes the speed resolution limited to 2%−3%. But this is not a real sacrifice since the inherent broad bandwidth of fs laser pulses will eventually limit the speed resolution achievable in TRPES experiments.

II. NEW APPARATUS

A. Velocity map imaging spectrometer

The newly constructed VMI spectrometer is very similar to the setup as described by Eppink and Parker [24], with necessary modifications suitable to 1 kHz repetition and fs time-resolved experiments. The apparatus consists of a source chamber and an interaction chamber, both differentially pumped, as shown in FIG. 1. The source chamber and the interaction chamber are evacuated with a 3200 and a 1000 L/s magnetically levitated turbo-molecular pump (Edwards, 3306c and 1003c), respectively, sharing a backing pump station (Pfeiffer, HiCube 80 Eco). The vacuum for both chamber with the molecular beam off are as good as 1×10^{-9} Torr. The source and interaction chambers are separated by a skimmer with a 1-mm diameter aperture (Beam Dynamics Inc.), which is mounted on a translatable gate-valve assembly [25]. With this design, the source chamber could be vented to atmospheric pressure while the interaction chamber maintains base vacuum. This design is practically important for experiments with liquid or solid samples which need to be loaded into the cartridge of the Even-Lavie pulsed valve. By this design, this can be done without the need for a time consuming pump-up of the interaction chamber before the experiments are restarted. A typical turnaround time

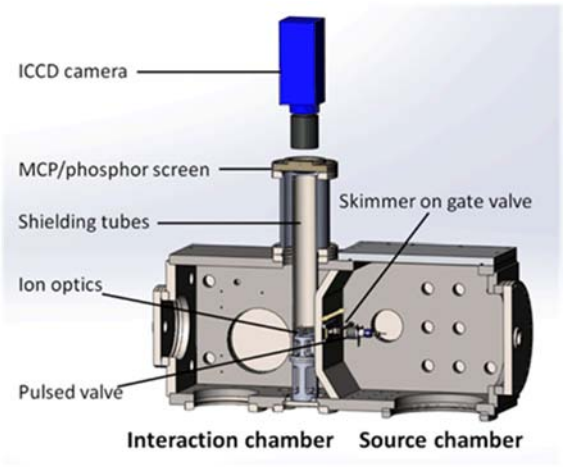

FIG. 1 Schematic view of the velocity map imaging spectrometer.

for sample replacement and subsequent recommencement of data acquisition is about 1.5 h.

The molecular beam is produced by expanding gas sample into vacuum through a pulsed valve [26] (Even-Lavie valve, 200 μm diameter conical nozzle) operating at 1 kHz. For gas samples or liquid samples with reasonable vapor pressure at room temperature, a prepared mixture of sample and carrier gas is used. While for liquid or solid samples with low vapor pressure, the samples are preloaded into the cartridge which is within the body of valve and then carrier gas flows through the cartridge before expanding into vacuum through the nozzle. The valve can be heated up to 250 °C to adjust the concentration of the sample in the mixture. The distance between the nozzle and the skimmer is adjustable from 20 mm to 120 mm. After passing through the skimmer, the molecular beam is intersected by laser beams at the center of ion optics which consists of three electrodes. The electrodes are 1-mm-thick stainless steel plates of 56 mm in diameter mounted with aluminum oxide spacers of about 5 mm in length (Kimball Physics Inc). The repeller electrode is a plate, while both the extractor and ground electrode have a 5-mm-diameter hole at the center. The ion optics could be used for ion or electron imaging by simply changing the polarity of the power supplies for them. The time-of-flight axis is perpendicular to the plane containing molecular and laser beams. The ion optics and the time-of-flight (TOF) path to the detector are shielded from the stray electric and magnetic fields by a stainless steel and a μ-metal shielding tubes. A 75-mm dual micro channel plate (MCP) detector backed by a P31 phosphor screen (Photek Limited, VID275. The decay time of P31 to 10% brightness quoted by Photek is 40 μs.) is mounted onto a flange at the end of the TOF tube. There is a 10-mm gap between the end of these shielding tubes and MCP detector to ensure adequate gas pumping in the region close to the detector. The distance

DOI:10.1063/1674-0068/30/cjcp1702018

from the interaction point to the front surface of the MCP detector is about 558 mm. The MCP plates and the phosphor screen are powered by a 3-channel high voltage power supply (Photek Limited, DPS3), with the back plate of MCP assembly gated with a high voltage gate unit (Photek Limited, GM-MCP). Charged particles impinging on the MCP/phosphor screen are recorded by an ICCD camera with a 1024×1024 pixel array (Princeton Instruments, Pi-max3 1024i). The intensifier of the ICCD camera is operated at a repetition rate of 1 kHz, fully compatible with the fs laser system. The intensifier is timed with the laser system and gated. The intensifier is only open when the ion or electron cloud impinges on the MCP/phosphor screen, greatly reducing the background. The accumulated signal on the CCD chip will be read out before getting saturated, typically at a rate of 10 Hz or even less, depending on the signal level. By this method, the 1 kHz imaging on the MCP/phosphor screen is collected with a high efficiency, without noise problem inherent to long exposure method which is often used when a low repetition rate CCD camera is used in a 1 kHz experiment. A photomultiplier tube (Hamamatsu, H10722-20) mounted beside the ICCD camera is used to record TOF spectrum of charged particles arriving at MCP/phosphor screen detector, by switching off the gate unit and running the detector at the DC mode.

B. Femtosecond laser system

The laser system, shown schematically in FIG. 2, consists of a fully integrated Ti:Sapphire oscillator/amplifier system (Coherent, Libra-HE), two commercial optical parametric amplifiers (OPAs, Coherent, OPerA-Solo) and a fourth harmonic generation (FHG) box. The regenerative amplifier delivers about 3.8 mJ/pulse at a repetition rate of 1 kHz, with a pulse duration slightly less than 50 fs and a central wavelength of 800 nm. The output of the amplifier is split into 4 beams, two of them with about 1.3 mJ/pulse, the third 0.9 mJ/pulse and the last 0.3 mJ/pulse. The first two are used to pump two OPAs. The outputs of OPAs are wavelength tunable from 240 nm to 2600 nm, with microjoule pulse energy level even at wavelengths of the lowest efficiency. The output of one of the OPAs is further mixed with the 0.3 mJ/pulse beam in a BBO crystal to push the wavelength down to 200 nm. The 0.9 mJ/pulse beam is used to pump the FHG box in which the fundamental is frequency doubled, tripled, and then quadrupled by a series of BBO crystals. Depending on the specific experiment, either the third harmonic or the fourth harmonic is used, with typical pulse energies of 12 and 1 μJ, respectively. There are two motorized high-performance travelling linear stage (Newport, M-ILS250HA), one between the amplifier and one of the OPAs and the other between the amplifier and the FHG box, which provide the capability to change

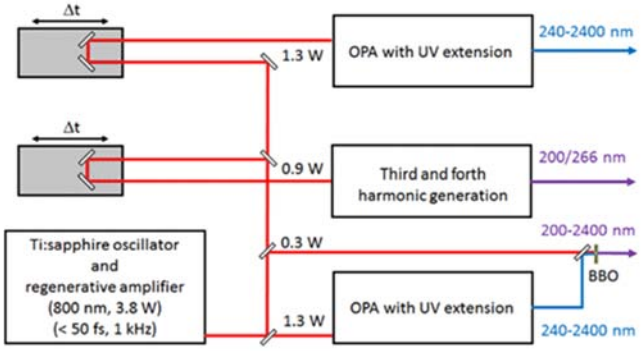

FIG. 2 Schematic overview of the femtosecond laser system.

the temporal delay between any two of the three arms with a minimum step size of 2 fs and a maximum delay of 1.5 ns. These laser beams are combined with one or two thin dichroic mirrors and focused into the VMI spectrometer where they intersected with the molecular beam at 90°.

C. Data acquisition program

A time-resolved photoelectron or photoion imaging experiment needs taking images at many different delays, including those with very small signal. Therefore, it usually takes many hours or even days to get enough statistics for data analysis. The data acquisition needs to be done by systematically changing the pump/probe delay back and forth many times in order to minimize the uncertainties caused by the variations in pulse energies of laser pulses, molecular beam intensity, pointing of laser beams, *etc.* A reliable and automated data acquisition program is therefore necessary.

We have developed such a program in LabVIEW environment. The main features are listed below: (i) Data acquisition parameters setting including the number of delays scanning, the number of laser shots at each delay in a delay scanning for pump/probe signal, the number of laser shots at each delay in a delay scanning for pump or probe only signal (single color signal is delay independent and subtracted in data analysis as background.), the delays (equally or non-equally spaced) where the images are taken. (ii) Automatically change the pump/probe delay by moving the motorized travelling linear stage and read the status of stage as feedback. (iii) Automatically block/unblock pump or probe laser beam using optical shutters. This provides the capability of taking signal and background alternatively at each delay. (iv) Real-time data analysis, including the reconstruction of the 3D distribution of charged particles from the 2D images [27], and the further derivation of the velocity and angular distributions. Two methods of reconstruction of the 3D distribution are implemented: one is the basis-set expansion method [28−30] and the other is similar to that proposed by Cho and

DOI:10.1063/1674-0068/30/cjcp1702018

Na [31] and Townsend and coworkers [21], but developed independently. (v) COG calculations [23] are also integrated into this program although it is disabled in the fs time-resolved experiments due to the limited resolution caused by the bandwidth of fs laser pulses.

III. EXPERIMENTAL RESULTS

A. Velocity calibration of VMI spectrometer

The velocity calibration of the apparatus was done by measuring the photoelectron image from multiphoton ionization of Xenon atom at 400 nm (second harmonic of the fundamental). The Xe beam was generated by expanding neat Xe of 5 bar using the Even-Lavie pulsed value operating at 1 kHz repetition rate. The raw photoelectron image accumulated over 0.2 million laser shots is shown in FIG. 3(a) after the subtraction of background which is taken with the laser and molecular beams temporally separated. The photoelectron 3D distribution is reconstructed using the β-basis expansion method [29] and the cut through the center of the 3D distribution is shown in FIG. 3(b). Integrating the 3D distribution over recoil angles gives the distribution of photoelectron along the radial direction, as shown in FIG. 3(c). The peaks in this distribution are readily assigned to photoelectron of Xe ionized with 4, 5 and 6 photons of 400 nm. There are two peaks correspond to 5 photons ionization process, resulting into the ground ($Xe^+(^2P_{3/2})$) and spin-orbit excited ($Xe^+(^2P_{1/2})$) cation, respectively. The kinetic energy of the photoelectron at each peak in this distribution is readily calculated. In FIG. 3(d), the square root of the kinetic energy of photoelectron at each peak is plotted against the radius (in pixel) of the corresponding ring in the image. This plot is very well fitted with a straight line crossing the ordinate at 0 which proves the VMI spectrometer is properly working [24]. Measurements at different voltages, with a fixed ratio between repeller and extractor electrodes were also performed (not shown) which proves that the VMI spectrometer works properly over a wide range of voltages.

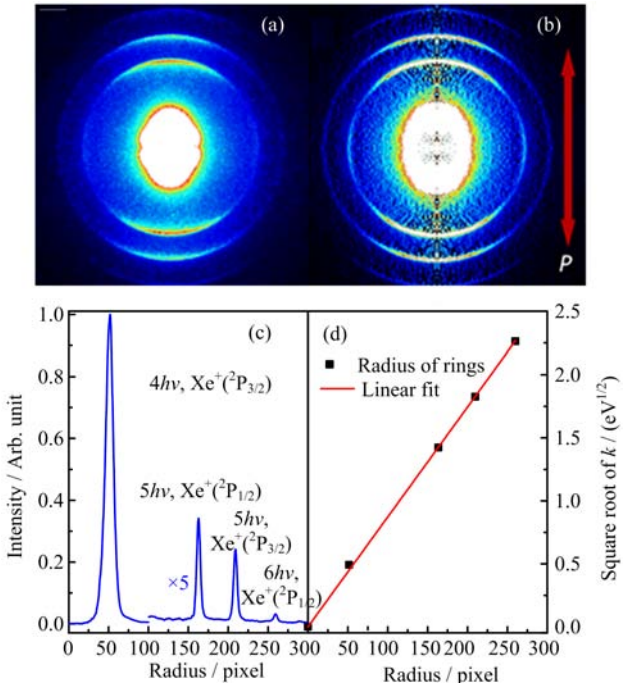

FIG. 3 (a) The raw photoelectron image from multiphoton ionization of Xe at 400 nm. (b) The cut through the center of the 3D distribution derived from (a) using p-Basex transformation method. (c) The speed distribution (in pixel unit) obtained from (b). (d) The square root of kinetic energy of electron *vs.* the radius of the rings in (b). The double arrow indicates the polarization direction of the laser pulse.

B. Femtosecond time-resolved experiment

In a test experiment, the TRVMI study of NH_3 photodissociation at 200 nm is performed [20, 32]. The time-resolved total kinetic energy release (TKER) spectrum obtained by imaging the H atom products provides rich information about the H-atom elimination and the coupling between the initially excited S_1 state and the ground state S_0 of NH_3.

The NH_3 molecular beam was generated by expanding a mixture of 1% NH_3 in He carrier gas of 3 bar using a pulsed valve. The pump laser was at 200 nm (~0.5 μJ/pulse) which excites NH_3 from the ground state to ν_2'=4 in the first electronically excited state ($\tilde{A}(^1A_2'')$) [33, 34]. The nascent H-atom products were detected using 2+1 resonance-enhanced multiphoton ionization (REMPI) at 243.1 nm (~6 μJ/pulse). By systematically changing the delay between the pump and probe lasers, the time-resolved TKER spectrum is derived. The H-atom signal with pump or probe laser only was also recorded and subtracted as background. The T_0 and the cross-correlation between pump and probe laser pulses were measured using the delay dependence of the total NH_3 cation yield which gave a cross-correlation of 200 fs. It has to be emphasized that while a resolution of 200 fs is sufficient for the current study a much short cross-correlation is expected if both laser pulses have been compressed with prism pairs.

In FIG. 4, the time-resolved TKER spectrum is shown. At negative delays where the probe pulse proceeds the pump pulse, there is no appreciable H^+ signal, suggesting the H^+ signal at positive delays is generated by the pump pulse (as neutral H atom) and then probed by the probe pulse. At t>0, the H^+ signal rises quickly and then approaches a plateau at 1 ps and remains constant beyond, indicative of a fast H atom elimination. A cut of this time- and energy-resolved distribution along the delay coordinate at 1 ps is also plotted beneath the 2D data, which represents the kinetic energy distribu-

DOI:10.1063/1674-0068/30/cjcp1702018

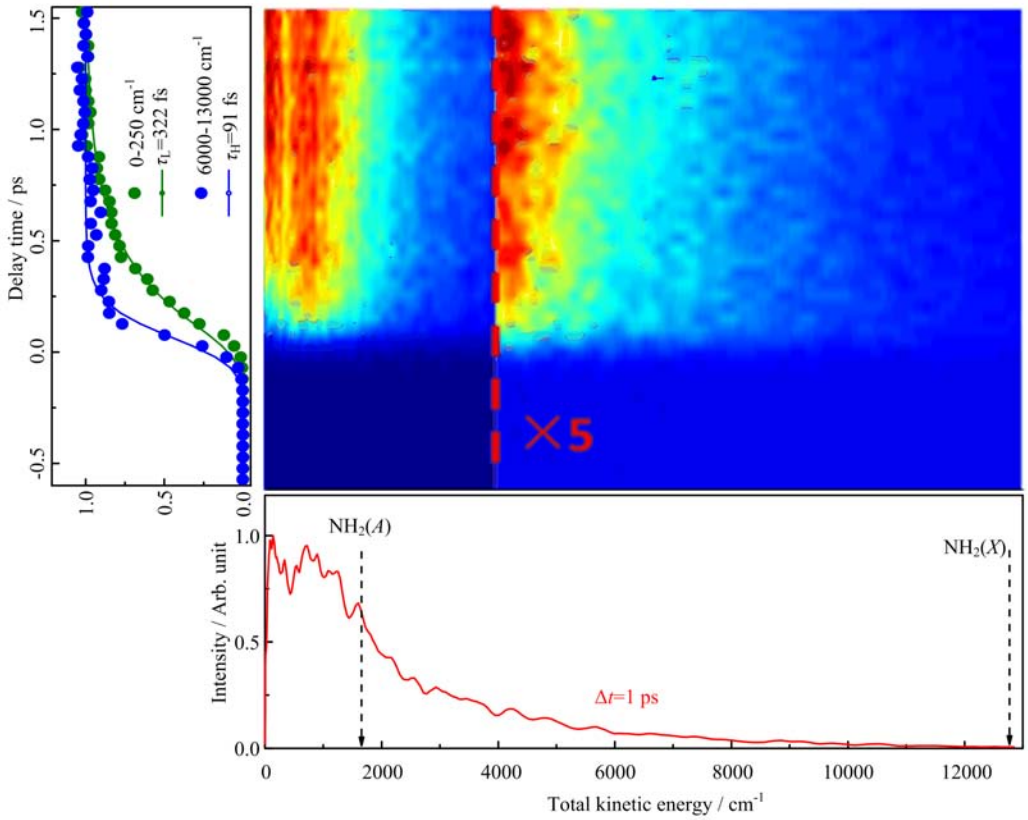

FIG. 4 Time-resolved TKER spectrum of the H+NH_2 fragments resulting from the photodissociation of NH_3 at 200 nm. The energetic limits for generating the ground state NH_2 $\widetilde{X}(^2B_1)$ and the first excited state NH_2 $\tilde{A}$ $(^2A_1)$ are indicated with dash arrows.

tion of H atom products when the reaction is completed entirely. At 200 nm, there are two channels open: the ground state NH_2 $\widetilde{X}(^2B_1)$ and the first excited state NH_2 $\widetilde{A}(^2A_1)$. The energetic limits for generating these two electronic states of NH_2 are indicated with dash arrows in FIG. 4. This distribution is very similar to that derived in previous photodissociation study [32], except a lower energy resolution in current study due to a much broader bandwidth of the fs laser pulses used here. Most interestingly, it is very clear from FIG. 4 that the appearance time of the H^+ signal is dependent on the kinetic energy of the H^+ ion: the H^+ ions with higher kinetic energies appear more promptly and those with lower kinetic energies relatively slowly, indicating that the H atoms produced at different delays have a different kinetic energy distributions. The H^+ signal transients integrated over a low and high kinetic energy ranges are plotted at the left figure which clearly shows the kinetic energy dependence of the time scales for H atom elimination. Using an error function, convoluted with the Gaussian cross-correlation between pump and probe pulse measured independently, these two curves are well fitted, giving appearance time of 322 and 91 fs for "slow" and "fast" H atom products, respectively. The implications of these observation to the photodissociation dynamics of NH_3 and the nonadiabatic coupling between the first excited and ground states are explained in detail in previous study [20] by Stavros and coworkers. We are not going to reiterate here.

IV. CONCLUSION

A new VMI spectrometer has been constructed for molecular reaction dynamics studies using a time-resolved photoelectron/ion spectroscopy method. By combining a kHz pulsed valve and an ICCD camera, this VMI spectrometer can be run at a repetition rate of 1 kHz, totally compatible with the fs Ti:Sapphire laser system, facilitating time-resolved studies in gas phase which are usually time-consuming. A fully automated data acquisition program was also developed for this TRVMI spectrometer. In a test experiment, TRVMI study of NH_3 photodissociation at 200 nm was performed. The time-resolved TKER spectrum of H+NH_2 products shows that the elimination time of the H products is clearly dependent on their kinetic energy, suggesting a rich dynamics in the photodissociation of NH_3. These results show that this new apparatus is a powerful tool for investigating the molecular reaction dynamics using time-resolved methods.

DOI:10.1063/1674-0068/30/cjcp1702018

V. ACKNOWLEDGMENTS

This work was supported by the National Basic Research Program of China (No.2013CB922200), the Ministry of Science and Technology of China (No.2012YQ12004704), and the National Natural Science Foundation of China (No.21573228).

[1] M. Dantus, M. J. Rosker, and A. H. Zewail, J. Chem. Phys. **87**, 2395 (1987).
[2] T. S. Rose, M. J. Rosker, and A. H. Zewail, J. Chem. Phys. **88**, 6672 (1988).
[3] A. H. Zewail, J. Phys. Chem. A **104**, 5660 (2000).
[4] J. H. D. Eland, *Photoelectron Spectroscopy*, 2nd Edn., Southampton: Butterworths, (1985).
[5] I. Fischer, D. M. Villeneuve, M. J. J. Vrakking, and A. Stolow, J. Chem. Phys. **102**, 5566 (1995).
[6] C. C. Hayden and A. Stolow, *in Photoionization and Photodetachment*, Vol.10A, C. Y. Ng Ed., Singapore: World Scientific Publishing Company, 91 (2000).
[7] W. Radlo, *in Photoionization and Photodetachment*, Vol.10A, C. Y. Ng Ed., Singapore: World Scientific Publishing Company, 127 (2000).
[8] K. Takatsuka, Y. Arasaki, K. H. Wang, and V. McKoy, Faraday Discuss. **115**, 1 (2000).
[9] D. M. Neumark, Annu. Rev. Phys. Chem. **52**, 255 (2001).
[10] T. Suzuki and B. J. Whitaker, Int. Rev. Phys. Chem. **20**, 313 (2001).
[11] T. Seideman, Annu. Rev. Phys. Chem. **53**, 41 (2002).
[12] K. L. Reid, Annu. Rev. Phys. Chem. **54**, 397 (2003).
[13] A. Stolow, Annu. Rev. Phys. Chem. **54**, 89 (2003).
[14] A. Stolow, A. E. Bragg, and D. M. Neumark, Chem. Rev. **104**, 1719 (2004).
[15] M. Wollenhaupt, V. Engel, and T. Baumert, Annu. Rev. Phys. Chem. **56**, 25 (2005).
[16] I. V. Hertel and W. Radloff, Rep. Prog. Phys. **69**, 1897 (2006).
[17] T. Suzuki, Annu. Rev. Phys. Chem. **57**, 555 (2006).
[18] A. Stolow and J. G. Underwood, *in Adv. Chem. Phys.* Vol.39, S. A. Rice Ed., New York: John Wiley & Sons, Inc., 497 (2008).
[19] G. Wu, P. Hockett, and A. Stolow, Phys. Chem. Chem. Phys. **13**, 18447 (2011).
[20] K. L. Wells, G. Perriam, and V. G. Stavros, J. Chem. Phys. **130**, 074308 (2009).
[21] R. A. Livingstone, J. O. F. Thompson, M. Iljina, R. J. Donaldson, B. J. Sussman, M. J. Paterson, and D. Townsend, J. Chem. Phys. **137**, 184304 (2012).
[22] T. Horio and T. Suzuki, Rev. Sci. Instrum. **80**, 013706 (2009).
[23] B. Y. Chang, R. C. Hoetzlein, J. A. Mueller, J. D. Geiser, and P. L. Houston, Rev. Sci. Instrum. **69**, 1665 (1998).
[24] A. T. J. B. Eppink and D. H. Parker, Rev. Sci. Instrum. **68**, 3477 (1997).
[25] A. Stolow, J. Vac. Sci. Technol. A **14**, 2669 (1996).
[26] U. Even, Adv. Chem. **2014**, 11 (2014).
[27] A. T. J. B. Eppink, S. M. Wu, and B. J. Whitaker, *in Imaging in Molecular Dynamics: Technology and Applications*, B. J. Whitaker Ed., Cambridge: Cambridge University Press, (2003).
[28] V. Dribinski, A. Ossadtchi, V. A. Mandelshtam, and H. Reisler, Rev. Sci. Instrum. **73**, 2634 (2002).
[29] G. A. Garcia, L. Nahon, and I. Powis, Rev. Sci. Instrum. **75**, 4989 (2004).
[30] F. Renth, J. Riedel, and F. Temps, Rev. Sci. Instrum. **77**, 033103 (2006).
[31] Y. T. Cho and S. J. Na, Meas. Sci. Technol. **16**, 878 (2005).
[32] J. Biesner, L. Schnieder, G. Ahlers, X. Xie, K. H. Welge, M. N. R. Ashfold, and R. N. Dixon, J. Chem. Phys. **91**, 2901 (1989).
[33] L. D. Ziegler, J. Chem. Phys. **82**, 664 (1985).
[34] V. Vaida, M. I. McCarthy, P. C. Engelking, P. Rosmus, H. J. Werner, and P. Botschwina, J. Chem. Phys. **86**, 6669 (1987).

DOI:10.1063/1674-0068/30/cjcp1702018